

We are IntechOpen, the world's leading publisher of Open Access books Built by scientists, for scientists

6,900

Open access books available

186,000

International authors and editors

200M

Downloads

Our authors are among the

154

Countries delivered to

TOP 1%

most cited scientists

12.2%

Contributors from top 500 universities



WEB OF SCIENCE™

Selection of our books indexed in the Book Citation Index
in Web of Science™ Core Collection (BKCI)

Interested in publishing with us?
Contact book.department@intechopen.com

Numbers displayed above are based on latest data collected.
For more information visit www.intechopen.com



Similariton-Based Spectral Interferometry for Signal Analysis on Femtosecond Time Scale

Levon Mouradian, Aram Zeytunyan and Garegin Yesayan
*Ultrafast Optics Laboratory, Faculty of Physics,
Yerevan State University,
Armenia*

1. Introduction

The *signal analysis problem on the femtosecond time scale* employs the powerful arsenal of contemporary optics, involving the methods of nonlinear and adaptive optics, Fourier optics and holography, spectral interferometry, etc. The nonlinear-optical techniques of FROG and its modifications [1], the most popular and commercialized, provide accurate and complete determination of the temporal amplitude and phase by recording high-resolution spectrograms, which are further decoded by means of iterative phase-retrieval procedures. The approach of *spectral interferometry (SI)* [2] and its developments to the methods of SPIDER [3], SPIRIT [4], and SORBETS [5] have the advantage of non-iterative phase retrieval. The recently developed and effectively applied MIIPS technique [6] operates with spectral phase measurement through its adaptive compensation up to transform-limited pulse shaping by using feedback from the SHG process. All these methods are based on the spectral phase determination, spectrum measurement, and reconstruction of a temporal pulse. The pulse direct measurement is possible by the transfer of temporal information to the space or frequency domain, or to the time domain with a larger - measurable scale. The time-to-space mapping through Fourier holography, implemented in real time by using a special multiple-quantum-well photorefractive device [7] or second-harmonic-generation crystal [8], provides a temporal resolution given by the duration of reference pulse. In an alternative approach, the $10^3\times$ up-conversion time microscope demonstrates a 300 fs resolution [9]. In the time-to-frequency conversion approach, the methods of optical frequency inter-modulation by sum-frequency generation [10,11] and electro-optical modulation [12-13] are limited to the picosecond domain. The technique of optical chirped-pulse gating [14] demonstrates sub-picosecond resolution. The method of pulse spectro-temporal imaging through temporal lensing is more promising, having as a principal limit of resolution the ~ 1 fs nonlinear response time of silica [15-20]. Its recent modifications, implemented in the silicon chip [21] and similariton-induced parabolic temporal lens [22], provide accurate, high-resolution direct measurement of a pulse in the spectrometer as in the femtosecond optical oscilloscope.

Many modern scientific and technological problems, such as revealing the character and peculiarities of nonlinear-dispersive similariton [23], studies of the nonlinear-dispersive regime of spectral compression and shaping of transform-limited rectangular pulses [24],

characterization of prism-lens dispersive delay line [25], etc, however, along with the amplitude information, demand also the phase information, possible through additional interferometric measurements, motivating the urgency of SI methods for the complete characterization of femtosecond signal. The *classic method of SI* is based on the interference of the signal and reference beams spectrally dispersed in a spectrometer, with the spectral fringe pattern caused by the difference of spectral phases [2]. The known spectral phase of the reference permits to retrieve the spectral phase of signal, and, together with the spectrum measurement, to recover the complex temporal amplitude of the signal through Fourier transformation. The setup of classic SI is rather simple, and the measurement is accurate as any interferometric one, but its application range is restricted by the bandwidth of the reference. The SI characterization of a signal that has undergone a nonlinear interaction with medium requires a special broadband reference to fully cover the broadened signal spectrum. To avoid this restriction, the self-referencing methods of spectral shearing interferometry are developed [3-5]. This improvement promotes the SI-methods to the class of the most popular and commercialized methods of accurate measurements on the femtosecond time scale, making them compatible with the FROG techniques [1], at the expense of a complicated optical arrangement. Our developed method of similariton-based SI, along with its self-referencing performance, keeps the simplicity of the principle and configuration of the classic SI [2].

Similaritons, pulses with the distinctive property of self-similar propagation, recently attract the attention of researchers, due to fundamental interest and prospective applications in ultrafast optics and photonics, particularly for high-power pulse amplification, optical telecommunications, ultrafast all-optical signal processing, etc [26,27]. The self-similar propagation of the high-power pulse with parabolic temporal, spectral, and phase profiles was predicted theoretically in the 90's [28]. In practice, the generation of such parabolic similaritons is possible in active fibers, such as rare-earth-doped fiber amplifiers [29-31] and Raman fiber amplifiers [32], as well as in the laser resonator [33]. The generation of parabolic similariton has been also proposed in a tapered fiber with decreasing normal dispersion, using either passive dispersion-decreasing fiber [34] or a hybrid configuration with Raman amplification [35]. Another type of similariton is generated in a conventional uniform and passive (without gain) fiber under the combined impacts of Kerr-nonlinearity and dispersion [23]. In contrast to the parabolic similariton with parabolic amplitude and phase profiles, this nonlinear-dispersive similariton has only parabolic phase but maintains its temporal (and spectral) shape during the propagation, as well. Our SI studies of this type of pulses [36,37] show the linearity of their chirp (parabolic phase), with a slope given only by the fiber dispersion. This property leads to the spectrotemporal similarity and self-spectrotemporal imaging of nonlinear-dispersive similariton, with accuracy given both by spectral broadening and pulse stretching. The relation of such a similariton with the flat-top "rectangular" pulse, shaped in the near field of nonlinear-dispersive self-interaction, leads to its important peculiarity: the bandwidth of nonlinear-dispersive similariton is given by the input pulse power, with slightly varying coefficients given by the input pulse shape [23, 38,39]. Both the parabolic similariton of active fiber and nonlinear-dispersive similariton of passive fiber are of interest for applications in ultrafast optics, especially for pulse compression [40,41] and shaping [42], similariton-referencing temporal lensing and spectrotemporal imaging [23], and SI [43]. The applications to ultrafast optics, however, demand the generation and study of broadband similariton. Particularly, the resolution of

the femtosecond oscilloscope, based on the similariton-induced parabolic lens, is given by the bandwidth of similariton [22], and the application range for similariton-based SI [43] is as large as broadband the similariton-reference is. The pulse compression ratio is also as high as the spectral broadening factor is [40,41]. Experimentally, our SI study permitted the complete characterization of the nonlinear-dispersive similariton of up to 5 THz bandwidths [36,37]. For broadband similaritons (of up to 50-THz bandwidths), we applied the chirp measurement technique through spectral compression and frequency tuning in the sum-frequency generation process [22,44,45].

In our method of *similariton-based SI*, the part of signal is injected into a fiber to generate the nonlinear-dispersive similariton-reference. The residual part of the signal, passing an optical time delay, is coupled with the similariton in a spectrometer. The spectral fringe pattern, on the background of the signal and similariton spectra, completely covers the signal spectrum, and the whole phase information becomes available for any signal. The known spectral phase of the similariton-reference allows to retrieve the signal spectral phase, and by measuring also the signal spectrum, to reconstruct the complex temporal amplitude of the signal through Fourier transformation. Thus, the method of similariton-based SI joins the advantages of both the classic SI [2] and spectral shearing interferometry [3-5], combining the simplicity of the principle and configuration with the self-referencing performance [46, 47]. Experimentally examining the similariton-based SI, we carried out the comparative measurements with a prototype of the femtosecond oscilloscope (FO) based on the pulse spectrotemporal imaging in the similariton-induced temporal lens. The resolution of such a similariton-based FO is given by the transfer function of the similariton's spectrum [22], and FO with a similariton-reference of the bandwidth of 50 THz bandwidths provides the direct measurement of temporal pulse in a spectrometer of 7 fs temporal resolution. In the comparative experiments, we demonstrate and study the methods of similariton-based SI and spectrotemporal imaging as two applications of similariton. The reference-based methods become self-referencing by the use of similariton. The results of the measurements carried out by similariton-based SI and FO are in quantitative accordance. The similariton-based spectrotemporal imaging has the advantage of direct pulse measurement leading to the development of a femtosecond optical oscilloscope, but it does not give phase information without additional interferometric measurement. The similariton-based SI provides the complete (amplitude and phase) characterization of femtosecond signal.

Concluding the chapter introduction, our studies on the generation of nonlinear-dispersive similaritons of up to 50 THz bandwidths, and their experimental characterization by means of the methods of SI and chirp measurement through the technique of frequency tuning in spectral compression process are presented below. Our studies state that only fiber dispersion determines the phase of broadband nonlinear-dispersive similariton. Afterwards, our demonstration and study of the similariton-based SI for femtosecond signal complete characterization and the comparative experiments with FO based on the similariton-induced temporal lens are presented, carried out together with theoretical check and autocorrelation measurements, evidencing the quantitative accordance and high precision of both the similariton-referencing methods of SI and temporal lensing.

Outlining this chapter, after a brief review of modern methods of signal analysis on the femtosecond time scale, we present our studies of the nature and peculiarities of similariton generated in passive fiber carried out by classic SI, then – research of broadband similariton

in view of problems of femtosecond signal analysis-synthesis, and finally – comparative studies on the development of novel method of self-referencing similariton-based SI.

2. Spectral interferometric study of nonlinear-dispersive similariton

In this section, our spectral interferometric studies for the complete characterization of the similariton generated in passive fiber due to the combined impacts of nonlinearity and dispersion are described. Studies of the generation of nonlinear-dispersive similariton of passive fiber, its distinctive properties, especially its origin, nature and relation with the spectron and rectangular pulses, and the temporal, spectral and phase features in view of potential applications are presented. The nonlinear-spectronic character of such a similariton, with the key specificity of linear chirping, leads to important applications to the signal analysis - synthesis problems in ultrafast optics.

The outline of this section is the following: first, a rough analytical discussion and numerical studies are given to reveal the features of nonlinear-dispersive similariton, afterwards, experiments for the spectral interferometric characterization of nonlinear-dispersive similariton are presented to demonstrate the peculiarities of similariton predicted by the theory, then the technique for the measurement of similariton chirp by the use of spectrometer and autocorrelator is described, and finally, the study of the bandwidth (and duration) rule of nonlinear-dispersive similariton is presented.

2.1 Similariton self-shaped (generated) in passive fiber

In a *rough analysis* of nonlinear-dispersive similariton, first we consider the pulse propagation through a pure dispersive medium. In the far field of dispersion a *spectron* pulse is shaped [23], which repeats its spectral profile, in the temporal analogy of the Fraunhofer zone diffraction, and therefore propagates self-similarly. Mathematically, the solution of the dispersion equation for temporal amplitude $A(f, t) = FT^{-1}[\tilde{A}(0, \omega)\exp(-i\beta_2 f \omega^2 / 2)]$ at the propagation distance $f \gg L_D$ obtains the form

$$A(f, t) \propto \tilde{A}(0, \omega)\exp(i\beta_2 f \omega^2 / 2)\Big|_{\omega=Ct} = \tilde{A}(0, \omega)\Big|_{\omega=Ct} \exp(iCt^2 / 2). \quad (1)$$

In Eq. (1), $\tilde{A}(\omega) \equiv FT[A(t)]$ is the complex spectral amplitude, FT – the operator of Fourier transformation, $C \equiv d\omega / dt \approx -[\phi''(\omega_0)]^{-1} = (\beta_2 f)^{-1}$ – chirp slope; $L_D \equiv (\beta_2 \Delta\omega_0^2)^{-1}$ – dispersive length, $\phi''(\omega_0)$ – second derivative of the dispersion-induced spectral phase $\phi(\omega)$ at the central frequency ω_0 , β_2 – coefficient of second order dispersion, and $\Delta\omega_0$ – input spectral bandwidth. The condition of temporal Fraunhofer zone, meaning enough large pulse stretching $s \equiv \Delta t / \Delta t_0 \approx \Delta\omega_0^2 / C \gg 1$, gives the $1/s \approx C / \Delta\omega_0^2$ precision of the spectron's spectrotemporal similarity $|A(f, t)| \propto \tilde{A}(0, \omega)\Big|_{\omega=Ct} = \tilde{A}(f, \omega)\Big|_{\omega=Ct}$. For a 100 fs pulse propagating in a standard single-mode fiber L_D is of ~ 10 cm, and at the output of 1-m fiber we will have pulse stretching of $s \approx f / L_D \sim 10$, and spectrotemporal similarity of spectron of the $1/s \sim 10\%$ precision.

For a nonlinear-dispersively propagating pulse, the nonlinear self-interaction broadens the spectrum and increases the impact of dispersion, leading to a higher-precision spectron-similariton shaping. Quantitatively, for 100-fs pulse radiation in a single mode fiber with

average power $p \sim 100$ mW at a 76 MHz repetition rate, the nonlinear interaction length $L_{NL} \equiv (\beta_0 n_2 I_0)^{-1}$ is much shorter than the dispersive one: $L_{NL} \sim 1$ cm \ll $L_D \sim 10$ cm. This allows us to roughly split the impacts of nonlinear self-interaction and dispersive deformation of the pulse, assuming that first we have pure nonlinear self-phase modulation of the pulse and spectral broadening, and afterwards pure dispersive stretching and dispersive-spectronic propagation. For the phase of output pulse, we have $\varphi_D(f, t) = Ct^2 / 2$, and an additional phase term φ_{NL} of $FT[A(f \sim L_{NL}, t)]|_{\omega=\gamma t}$, come from the pulse initial propagation step of nonlinear self-interaction. Assuming it parabolic at the central energy-carrying part of the pulse at the propagation distances of $\sim L_{NL}$, we have the phase $\varphi_{NL}(f, t) = C_{NL}^{-1} \omega^2 / 2|_{\omega=\gamma t} = (C^2 / C_{NL})t^2 / 2$, with $C_{NL} \equiv \varphi_{NL}''$. For the overall output phase $\varphi_{\Sigma} = \varphi_D + \varphi_{NL}$, we have $\varphi_{\Sigma}(z, t) = Ct^2(1 + C / C_{NL}) / 2$. Considering the nonlinear spectral broadening and dispersive pulse stretching factors ($b \equiv \Delta\omega / \Delta\omega_0$ and $s \equiv \Delta t / \Delta t_0$), we have for the nonlinear, dispersive, and overall chirp slopes at the output, respectively: $C_{NL} = \Delta\omega / \Delta t_0 = \Delta\omega_0^2 b$, $C = \Delta\omega_0 / \Delta t = \Delta\omega_0^2 / s$, and $C_{\Sigma} = C(1 + C / C_{NL}) = C[1 + (sb)^{-1}]$. Since $C / C_{NL} = (sb)^{-1}$, for spectral broadening $b \sim 10$ and pulse stretching $s \sim 10$ ($\Delta t_0 \sim 100$ fs, $p \sim 100$ mW average power at a 76 MHz repetition rate, $f \sim 1$ m of fiber), we will have $C_{\Sigma} = C(1 + C / C_{NL}) \approx C$, with the accuracy of $C / C_{NL} \sim 1\%$.

Thus, for the femtosecond pulse nonlinear-dispersive self-interaction at $f \sim 1$ m of fiber, we have spectron of $\sim 1 / sb = C / \Delta\omega^2 \sim 1\%$ precision. Considering the key peculiarity of the nonlinear-dispersive spectron-similariton, that practically the fiber dispersion determines the chirp slope, we can describe it following way:

$$A(f, t) \propto \tilde{A}(f, \omega)|_{\omega=Ct} \exp(iCt^2 / 2). \quad (2)$$

Another interesting issue is the relation of nonlinear-dispersive similariton with the rectangular pulses, shaped due to the pulse nonlinear-dispersive self-interaction at the fiber lengths $f \sim 2\sqrt{L_D L_{NL}}$. For such nonlinear-dispersive rectangular pulses, the temporal stretching and spectral broadening are up to $\Delta t \approx 2\Delta t_0$ and $\Delta\omega \approx 2\Delta\omega_0(L_D / f)$, respectively, since the pulse optimal compression ratio is $\Delta t_0 / \Delta t_c \approx \sqrt{L_D / L_{NL}} / 2 = L_D / f$, and $\Delta t_0 / \Delta t_c \approx 2\Delta\omega / \Delta\omega_0$. Thus, in this case the chirp slope obtains the value $C = \Delta\omega / \Delta t \approx (2\Delta\omega_0 L_D / f) / (2\Delta t_0) = (\beta_2 f)^{-1}$. Therefore, during the pulse nonlinear-dispersive self-interaction in fiber, the chirp slope becomes equal to the one of pulse dispersive propagation $C \approx (\beta_2 f)^{-1}$, starting from the fiber lengths $f \sim 2\sqrt{L_D L_{NL}}$, and nonlinear-dispersive rectangular pulses can be considered as an earlier step of the shaping of nonlinear-dispersive similariton.

Summarizing our rough analysis, we can expect the spectronic nature of nonlinear-dispersive similariton of passive fiber, its spectrotemporal similarity and imaging with the accuracy $\sim 1 / sb = C / \Delta\omega^2$, and with the scaling coefficient of the chirp slope $C \approx (\beta_2 f)^{-1}$, given by dispersion only.

To check the terms and conclusions of the rough analytical discussion above, a quantitative analysis of the process is carried out through *numerical modeling* based on the complete wave pattern. The mathematical description of the pulse nonlinear-dispersive self-interaction in

fiber is based on the standard nonlinear Schrödinger equation (NLSE) with the terms of Kerr nonlinearity and second-order dispersion, adequate to the pulse durations of ≥ 50 fs [23]. The split-step Fourier method is applied to solve the NLSE. In simulations, the pulse propagation distance is expressed in dispersive lengths L_D ($L_D \sim 10$ cm for 100-fs input pulses); the power of radiation in fiber is given by the nonlinear parameter $R \equiv L_D / L_{NL} = (\beta_2 \Delta \omega_0^2)^{-1} \beta_0 n_2 I_0 \sim I_0$ ($p = 100$ mW average power of a 100-fs pulse radiation at a 76 MHz repetition rate in a standard single-mode fiber corresponds to $R = 6$; $p \leq 100$ uW is adequate to the pulse pure dispersive propagation of $R = 0$). The dimensionless running time t and centralized frequency Ω are normalized to the input pulse duration Δt_0 and bandwidth $\Delta \omega = 1 / \Delta t_0$, respectively.

Fig. 1 and 2 show the dynamics of similariton shaping: pulse (top row), chirp (middle row) and spectrum (bottom row) are shown during the pulse propagation in fiber. Fig. 1 illustrates the first step of nonlinear-dispersive self-interaction when, typically, rectangular pulses are shaped, and Fig. 2 shows the step of similariton shaping. The spectral broadening and decreasing of the pulse peak power lead to the “activation” of dispersion; the pulse obtains a linear chirp (parabolic phase), and the self-spectrotemporal similarity of nonlinear-dispersive similariton takes place (Fig. 2).

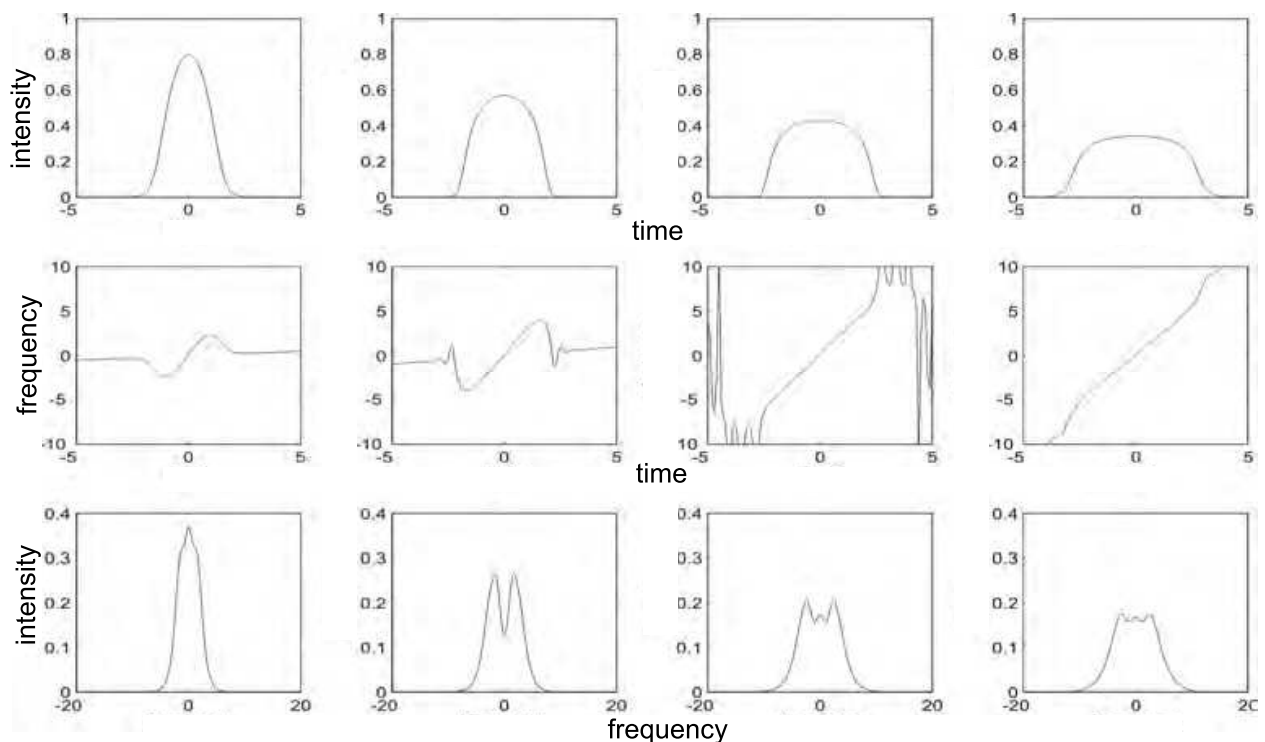


Fig. 1. Shaping of rectangular pulses ($R = 30$). From left to right: pulse evolution in fiber for $f / L_D = 0.1; 0.2; 0.3; \text{ and } 0.4$. From top to bottom: pulse, chirp, and spectrum.

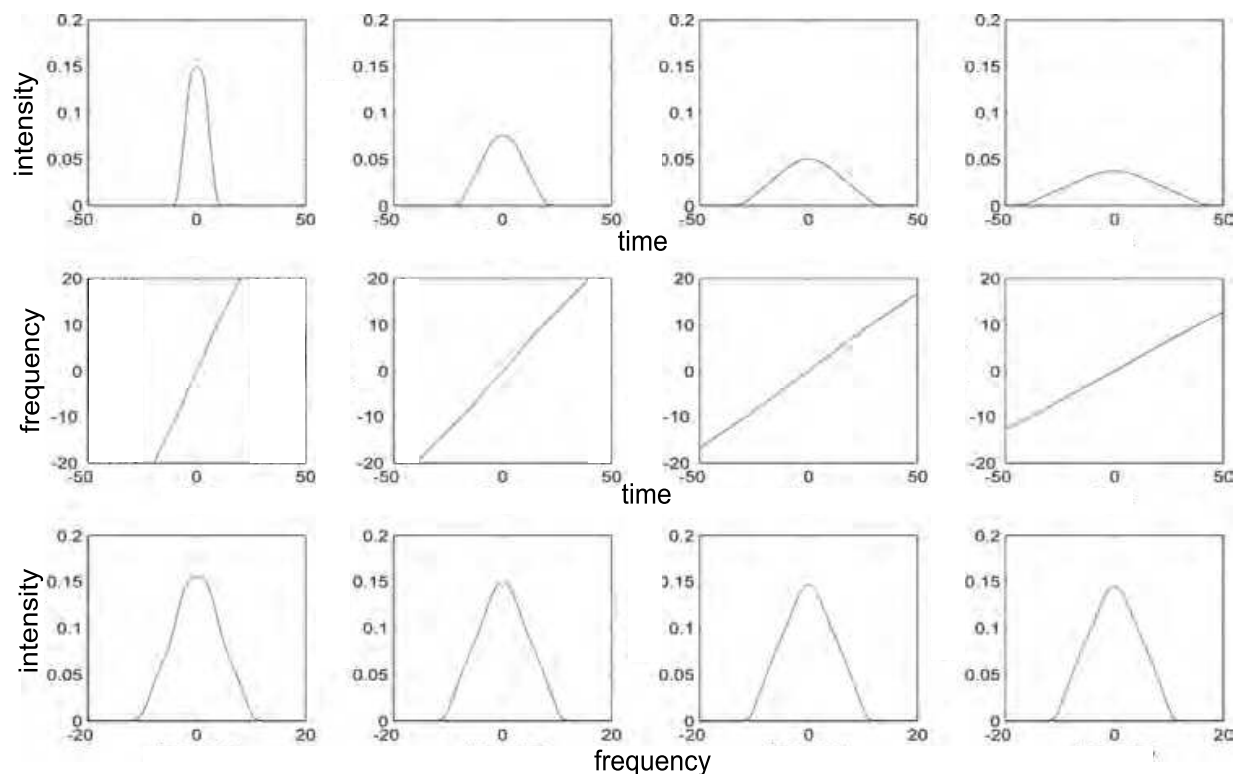


Fig. 2. Shaping and evolution of nonlinear-dispersive similariton in the fiber ($R = 30$). From left to right: $f / L_D = 1; 2; 3; 4$. From top to bottom: pulse, chirp, and spectrum.

Our simulations show that even in case of pulses with complex initial forms the output pulse has nearly parabolic form at its central energy-carrying part. The irregularities of the temporal and spectral profiles are forced out to the edges during the nonlinear-dispersive self-interaction, and pulse and spectrum become more and more parabolic. However, the pulse dispersive stretching decreases its peak intensity, finally minimizing the impact of nonlinear self-phase modulation. The spectrum does not change any more and the further alteration of the pulse shape has a dispersive character only.

It is important that our simulations for the nonlinear-dispersive similariton at a given fiber length and different power values confirm also the prediction of the analytical discussion: the output chirp slope is practically independent of the input pulse intensity, and depends only on the fiber length. The increase of input pulse power leads to the spectral broadening and temporal stretching of pulse, keeping the chirp coefficient unchanged: the chirp slope is the same in all cases, even in case of pulse pure dispersive propagation. It allows extracting the full information on the nonlinear-dispersive similariton having the spectrum and fiber length. This statement is checked for sufficiently powerful pulses, when the character of pulse self-interaction is nonlinear-dispersive (but not pure dispersive), and the result is the same: the chirp slope is independent of the power.

We studied also the chirp of nonlinear-dispersive similariton versus the chirp of input pulse: the chirp slope of similariton is practically constant, when the pulse intensity is high enough. In case of the dispersive propagation, the induced chirp simply imposes on the initial chirp according to Eq. (1). In case of nonlinear-dispersive propagation, the chirp "forgets" about the initial chirp according to analytic discussion above: it becomes independent of the input chirp according to Eq. (2).

2.2 Spectral interferometric characterization of nonlinear-dispersive similariton

We carried out experimental studies to check-confirm the predictions of our rough discussion and numerical analysis above. We applied the classic method of SI [2] to completely characterize and study the generation process and peculiarities of nonlinear-dispersive similariton of a passive fiber.

Fig. 3 schematically illustrates our experiment. Using a Mach-Zender interferometer, we split the input radiation of a standard Coherent Verdi V10-Mira 900F femtosecond laser system into two parts.

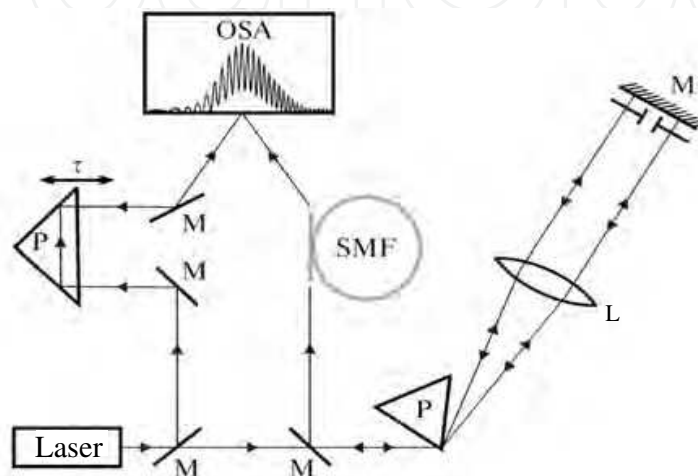


Fig. 3. Schematic of the experiment. Laser – Coherent Verdi V10-Mira 900F femtosecond laser system, M – mirrors, P – prisms, L – lens, OSA – optical spectral analyzer, and SMF – single-mode optical fiber.

The low-power pulse serves as a reference. For the high-power pulse, first we filter its spectrum of the bandwidth $\Delta\lambda = 11$ nm down to the value $\Delta\lambda = 2$ nm. We use standard polarization-preserving fibers Newport F-SPF @820 nm and ThorLabs HP @ 780 nm of different lengths – 1 m, 9 m, and 36 m. The spectra of the pulses at the output of fiber are broadened, however, the spectrum of the reference pulse covers them completely. This allows measuring the spectral phase of similariton within the whole range of its spectrum. The spectral interferometric fringe pattern is recorded by an optical spectrum analyzer (OSA Ando 6315), and the spectral phase is retrieved. Having the spectrum and retrieved spectral phase, the temporal profile of the similariton is reconstructed by Fourier transformation.

The performance of the experiment is given schematically in Fig. 4 by means of the spectrograms of relevant steps. Fig. 4(a) shows the spectrum of the laser pulse, (b) is the spectrum of spectrally filtered and shaped pulse, (c) is the spectrum of nonlinear-dispersive similariton and (d) is the SI fringe pattern. Fig. 4(e) shows the measured spectral phases of the similaritons generated from different input pulses. The spectral phases are parabolic ($\phi = -\alpha\omega^2 / 2$) and their coefficients α have nearly the same values in all cases of dispersive and nonlinear-dispersive propagations: $\alpha = 0.32$ ps² for the pure dispersive propagation of single-peak pulse, and 0.33 ps², 0.328 ps², 0.35 ps² for the nonlinear-dispersive propagations of single-, double- and distant double-peak pulses, respectively. The parabolic phase (linear chirp) leads to the self-spectrotemporal imaging of similariton. The accuracy of imaging

increases with the decreasing of the chirp slope, which is approximately equal to $C \approx \alpha^{-1}$. Fig. 4 and 5 illustrate the typical behavior of nonlinear-dispersive similariton in case of $f = 9$ m.

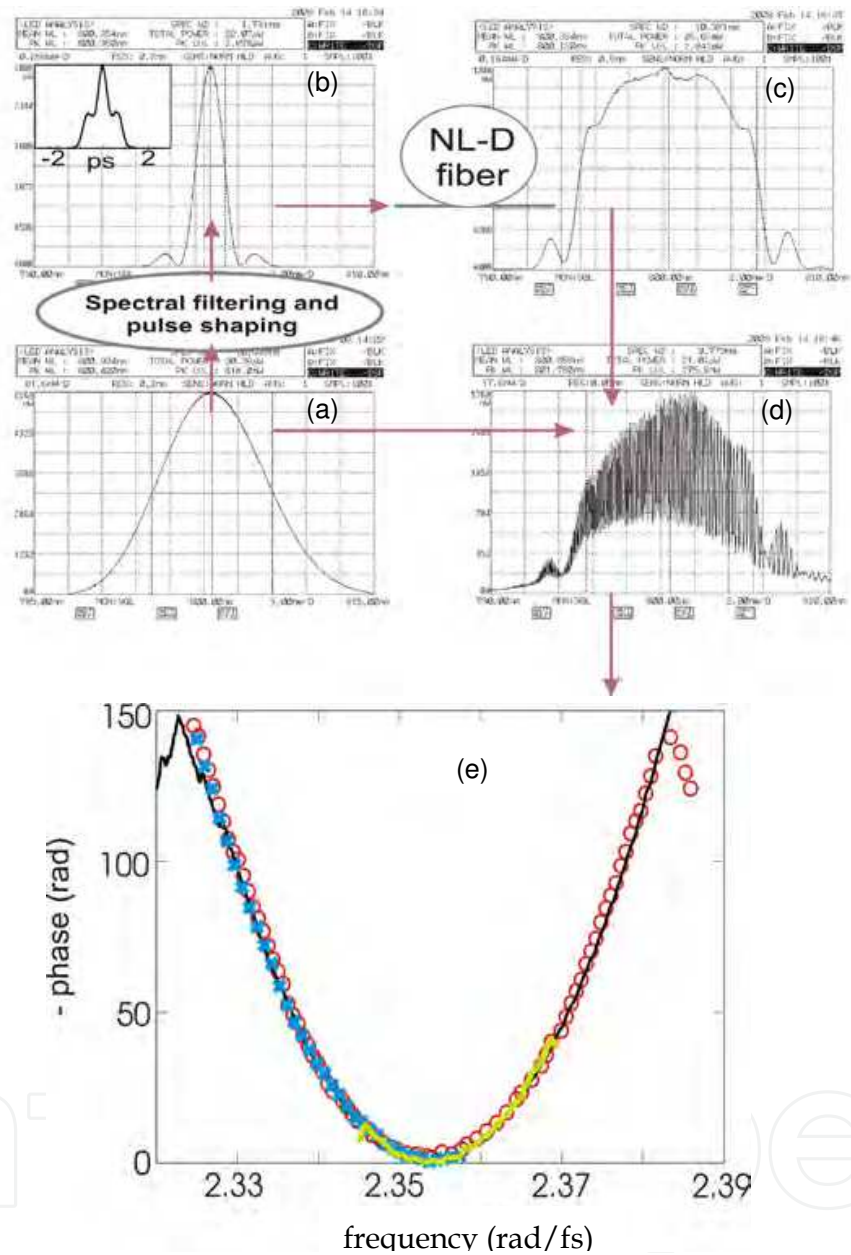


Fig. 4. (a-d) Schematic of the experiment given by the spectrograms of the relevant steps; (e) spectral phases of nonlinear-dispersive similaritons generated from input single- (thin black line), double- (red \circ) and distant double-peak (blue \times) pulses in comparison with the one for pure dispersively propagated single-peak pulse (thick yellow line).

Having the spectral phase and spectral profile, the temporal profile of nonlinear-dispersive similariton is retrieved. Fig. 5 shows the spectral and temporal profiles of the similaritons with the spectral phases of Fig. 4(e). The black curves are the spectra and the gray-dotted curves are the pulses. They coincide with each other, that is, takes place the self-

spectrotemporal imaging of nonlinear-dispersive similariton. A good spectrotemporal similarity is seen in case of input single-peak pulse (a). For the input double-peak pulse of (b), the matching between the spectral and temporal profiles of similaritons is qualitative only. To obtain a quantitative agreement, one must use a longer fiber, increasing the α coefficient: the spectral and temporal profiles of similaritons practically coincide for the thick orange line of (b), showing the temporal profile of similariton for the increased α coefficient.

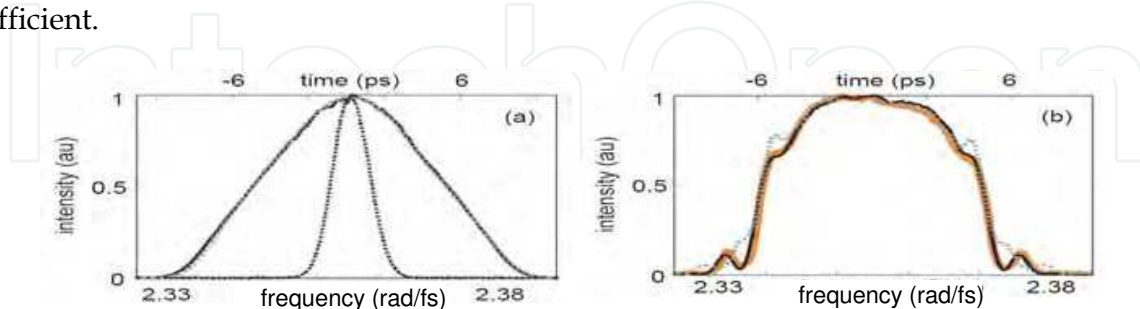


Fig. 5. Self-imaging of nonlinear-dispersive similaritons generated from input (a) single-, and (b) double-peak pulses. Black solid curves show the spectra of nonlinear-dispersively propagated pulses (the black dotted one of (a) stands for pure dispersively propagated pulse), gray dotted lines show the retrieved temporal profiles. The thick orange curve of (b) shows the temporal profile of similariton for 4α increased coefficient of spectral phase.

To show the relation between the nonlinear-dispersive similariton and the rectangular pulse of fiber, spectral interferometric measurements are carried out using a short fiber ($f = 1$ m). Fig. 6 illustrates the shaping of a rectangular pulse in a nonlinear-dispersive fiber.

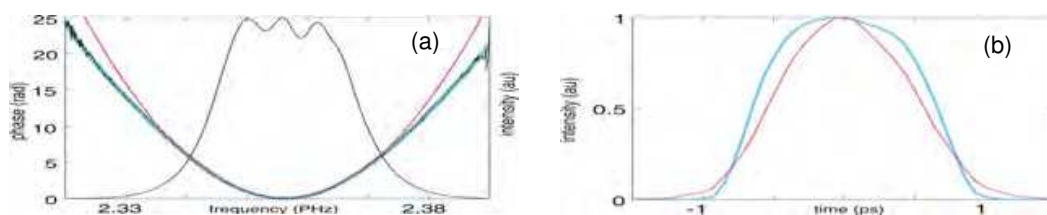


Fig. 6. (a) Spectrum of nonlinear-dispersive rectangular pulse with the relevant spectral phase (black solid line) and fitted parabola (pink). The blue line is a high-order polynomial fit. (b) Temporal profile of the rectangular pulse (blue) in comparison with the pulse retrieved by the fitted parabolic spectral phase (pink).

Here the black curves are the spectrum and spectral phase measured, the blue curve is a high-order polynomial fit and the pink is a fitted parabola. The measured spectral phase has a parabolic shape only at the central energy-carrying part of spectrum. Deviation from the parabola at the wings leads to the shaping of a rectangular pulse shown in Fig. 6(b) with the blue curve. Even in this case the chirp slope at the central energy-carrying part of the pulse/spectrum is also determined only by the fiber length ($\alpha = 0.0465$ ps²). The pink curve of Fig. 6(b) is the retrieved pulse by the fitted parabolic spectral phase.

The complete and precise SI study confirmed the principal description of nonlinear-dispersive similariton by Eq. (2), leading to its self-spectrotemporal similarity and imaging by the scaling coefficient of the chirp slope $C = (\beta_2 z)^{-1}$. This allows carrying out the

similariton chirp studies by a simpler way of the spectrum and autocorrelation track measurements, and afterwards calculation of the spectrum autocorrelation. The comparison of the measured and calculated autocorrelations extracts the chirp slope. A good accordance between the chirp slope values measured by this and SI methods occurs. This simple method permits checking easily the results on similariton chirp numerical study. The experimental results, in agreement with the theory, show that the chirp slope of nonlinear-dispersive similariton is practically independent of the input pulse phase modulation in a wide range of $\alpha_0 \Delta \omega_0^2$ from -3 to +3.

Taking into account the relation between nonlinear-dispersive similariton and rectangular pulse discussed, it seems reasonable to expect that the *bandwidth of similariton* is equal to the one for rectangular pulse. To determine the bandwidth (and afterwards the duration) of nonlinear-dispersive similariton, the relation for the pulse optimal compression can be used [23]. This gives the following relation for the spectral broadening of nonlinear-dispersive similariton: $b \equiv \Delta \omega / \Delta \omega_0 \approx \sqrt{R} \equiv \sqrt{L_D / L_{NL}} = k \sqrt{W / \Delta t_{in}} / \Delta \omega_0 = k \sqrt{P} / \Delta \omega_0$, where P is the input pulse power, Δt_{in} - input pulse duration, $W = p / v$ - pulse energy, p - average power of pulse radiation with a repetition rate v , and $k \equiv \sqrt{n_2 \beta_0 (\beta_2 S)^{-1}}$ is a coefficient given by the fiber parameters (n_2 - coefficient of the Kerr nonlinearity, $\beta_0 = 2\pi / \lambda_0$ - wave number, β_2 - group-velocity dispersion coefficient, S - fiber mode area). This thesis (Fig. 7) is checked numerically (a) and experimentally (b). The confirmation of the truthfulness of the brief discussion above gives the following rule for the $\Delta \omega$ bandwidth and Δt duration of nonlinear-dispersive similariton:

$$\Delta \omega = k \sqrt{P}, \quad \Delta t = \Delta \omega / C = k \beta_2 f \sqrt{P}. \tag{3}$$

For comparison, the spectral bandwidth of the similariton generated in a fiber amplifier is $\Delta \omega(z) = [(g \beta_0 n_2 P W) / (2 \beta_2^2 S)]^{1/3} \exp(gz / 3)$, where W and P are the input pulse energy and power, and g is the gain coefficient [31].

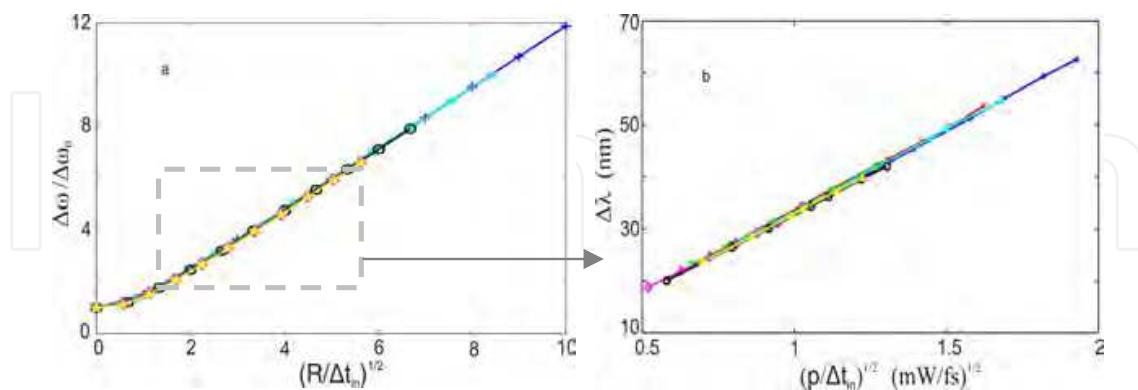


Fig. 7. (a) Simulation: spectral broadening versus R ; (b) Experiment: similariton bandwidth $\Delta \lambda$ versus $(p / \Delta t_{in})^{1/2}$. Blue lines correspond to the transform-limited pulse of 100 fs duration, red and cyan - to 140 fs pulse, green and black - to 225 fs pulse, magenta and yellow - to 320 fs pulse. Red, green and magenta are related to pulses stretched in a medium with normal dispersion, and cyan, black, and yellow - to pulses stretched in a medium with anomalous dispersion.

This revealed property of nonlinear-dispersive similariton of Eq. (3) can be used for the measurement of femtosecond pulse duration, alternatively to the autocorrelation technique.

Concluding, our spectral interferometric studies demonstrate the following properties of nonlinear-dispersive similariton generated in a passive fiber:

- linear chirp, with a slope given only by the fiber dispersion and independent of the amplitude, chirp and power of the input pulse;
- relation with the rectangular pulse of nonlinear-dispersive fiber;
- property of spectrotemporal similarity / self-spectrotemporal imaging, with accuracy determined by spectral broadening and pulse stretching together;
- only initial pulse power determines the spectral bandwidth of similariton.

3. Broadband similariton for femtosecond signal analysis and synthesis

The applications to ultrafast optics demand the generation and study of *broadband similariton* [43,44]. Particularly, the pulse compression ratio is as high as the spectral broadening factor is [41], the resolution of the femtosecond oscilloscope, based on the similariton-induced parabolic lens is given by the bandwidth of similariton [22], and for the similariton-based SI, the application range is as large as broadband the similariton-reference is [43,46].

In this section, our studies on the generation and characterization of a broadband, 50-THz bandwidth nonlinear-dispersive similariton are presented with the objective to reveal its distinctive properties in view of its applications to the signal synthesis and analysis problems on the femtosecond time scale. According to the spectral-interferometric characterization of nonlinear-dispersive similariton of the bandwidths of 5 THz ($\Delta\lambda \sim 10$ nm at $\lambda \sim 800$ nm), it is described by Eq. (2), or for its slowly varying amplitude $A(f,t)$ and phase $\varphi_f(f,t)$ we have:

$$A(f,t) \propto \tilde{A}^*(f,\omega)|_{\omega=Ct}, \varphi_f(t) = -\phi_f(\omega)|_{\omega=Ct} = \beta_2 f \omega^2 / 2|_{\omega=Ct} = Ct^2 / 2. \quad (2')$$

For comparison, the spectron pulse has the same dispersion-induced phase [Eq. (1)]. The applications of similariton demand to check and generalize this key peculiarity for broadband pulses.

First, the *numerical modeling* is carried out to have the complete physical pattern and reveal the distinctive peculiarities of the generation and propagation of broadband similariton. The mathematical description, based on the generalized nonlinear Schrödinger equation, considers the high-order terms of third-order dispersion (TOD), shock wave (self-steepening) and delayed nonlinear response (related to the Raman gain), together with the principal terms of self-phase modulation and second order dispersion (SOD) [44,47]. The split-step Fourier method is used in the procedures of numerical solution of the equation in simulations for 100-fs pulses of a standard laser with up to 500 mW of average power at a 76 MHz repetition rate (70 kW of peak power) in a few meters of standard single-mode fiber (losses are negligible). Simulations in these conditions show that the high-order nonlinear factors of shock wave and delayed nonlinear response do not impact on the process under study; however, the impact of TOD is expressed in the generated broadband similaritons of

50 THz bandwidth. It is conditioned by the physical pattern of the process: the nonlinear self-interaction of powerful pulses leads to large spectral broadening (with the factor of $b \sim 10$ just at the first ~ 1 cm of propagation in fiber, in our case), substantially increasing the impact of dispersion (with the factors of $b^2 \sim 100$ for SOD, and $b^3 \sim 1000$ for TOD), resulting in the pulse stretching and peak intensity decreasing (with the factor of $b^2 \sim 100$), and thus essentially decreasing and blocking out the high-order nonlinear effects. The impact of high-order nonlinear effects can be significant in case of high-power pulse propagation in low-dispersion fibers, e.g., for photonic crystal fibers with all-normal flattened dispersion, where a longer and more efficient nonlinear self-interaction results in the generation of octave spanning supercontinuum [48].

The numerical analysis shows that the fiber TOD is expressed additively in the $\phi(f, \omega)$ and $\phi(f, t)$ parabolic spectral and temporal phase profiles due to its small impact as compared to the SOD, and its value is the same for the nonlinear-dispersive similariton and the spectron pulse of pure dispersive propagation:

$$\Delta\phi(f, t) \approx \Delta\phi(f, \omega)|_{\omega=Ct} = -\frac{\beta_3 f}{6} \omega^3 \Big|_{\omega=Ct} \approx -\frac{\beta_3}{6\beta_2^3 f^2} t^3, \quad (4)$$

where β_3 is the TOD coefficient. The precision of Eq. (4) is of $\sim 4\%$, according to the simulations for the SOD and TOD coefficients of fused silica ($\beta_2 = 36.11 \text{ fs}^2/\text{mm}$ and $\beta_3 = 27.44 \text{ fs}^3/\text{mm}$). Thus, the chirp measurement of broadband similariton becomes urgent, since it gives the TOD of fiber and permits to generalize the description of Eq. (2'). The SI study permitted the complete characterization of nonlinear-dispersive similariton of up to 5 THz bandwidths [23]. For broadband similaritons (of up to 50-THz bandwidths), the chirp measurement technique through spectral compression and frequency tuning in the sum-frequency generation process is applied [44,45].

In the *experiment*, a broadband nonlinear-dispersive similariton of 50-THz FWHM-bandwidth is generated in a piece of passive fiber and the chirp measurement is carried out through frequency tuning in the SFG-spectral compression process [44-47]. Fig. 8 shows the schematic of the experimental setup. The Coherent Verdi V10 + Mira 900F femtosecond laser system is used, with the following parameters of radiation: 100 fs pulse duration, 76 MHz repetition rate, 1.6 W average power, 800 nm central wavelength. Beam-splitter (BS) splits the laser radiation into high- and low-power parts (80%+20%). The high-power pulse (100 fs FWHM-duration and pulse energy of up to 7 nJ, corresponding to 70 kW peak power) is injected into a standard single-mode fiber (1.65 m Newport F-SPF PP@820 nm) by means of a $10\times$ microscope objective and a broadband nonlinear-dispersive similariton is generated.

Fig. 9(a) shows the spectrum of 107-nm (50 THz) FWHM-bandwidth similariton, recorded by the optical spectrum analyzer Ando 6315 (OSA). This spectral profile represents the spectrotemporal image of the generated similariton in the approximation of its linear chirp. The asymmetry in this spectrotemporal profile evidences the impact of TOD. Although the initial pulse asymmetry can also cause the spectral asymmetry in the near field of dispersion, typically for the picosecond-scale experiments, the impact of the possible

asymmetry of the initial laser pulse on the spectrotemporal shape of similariton becomes insignificant, according to our simulations.

For the characterization of broadband similariton, its intensity profile can be measured by means of the cross-correlation technique, using the SFG-interaction of similariton with the laser pulse (as a reference). A spectral detection of the SFG-signal will give also information on the chirp of similariton, modifying the cross-correlation technique to the cross-correlation frequency-resolved optical gating (XFROG) [49,50]. Our additional modification is the use of a dispersively chirped reference pulse, which provides a spectrally compressed SFG-signal in a wider spectral range, and thus, more efficient measurement [22,44]. Experimentally, the low-power pulse is directed into the dispersive delay line with anomalous dispersion (D-line; conventional prism compressor consisting of a 3.5-m separated SF11 prism pair with a reverse mirror) and stretch it 22 times, resulting in the pulse autocorrelation duration of 3.1 ps. Then, using a lens, we direct the similariton and the dispersively stretched pulse to the nonlinear β -barium borate crystal (BBO, type 1 - ooe, 800 nm operating wavelength) to have SFG-spectral compression. The SFG-interaction of up- and down-chirped pulses results in the chirp cancellation and spectral compression, and a temporal delay between these two pulses leads to the frequency shift of the SFG-signal, according to the concept of the temporal lens [22]. In the experiment, the temporal delay is provided by shifting the reverse mirror of the D-line and recording the relevant SFG-compressed spectra by OSA. Measurements with D-line and without it are carried out, replacing the D-line with a simple temporal delay (TD), to compare the techniques of SFG-spectral compression and XFROG. Fig. 9(b) shows the relevant 3D frequency tuning patterns for the chirp measurement.

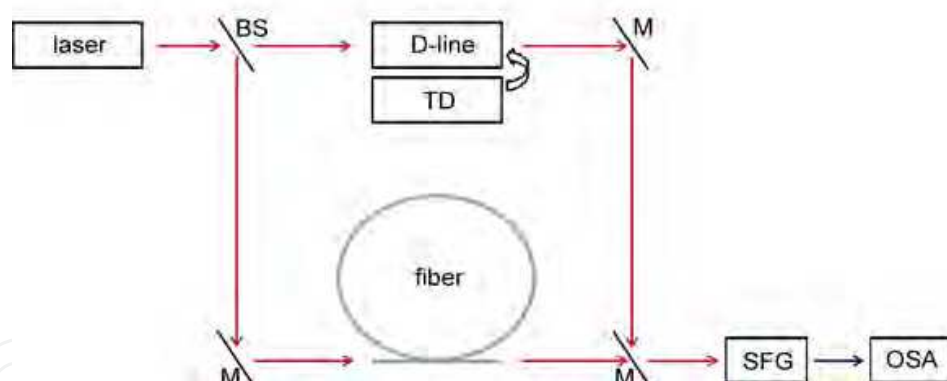


Fig. 8. Schematic of experimental setup: laser – Coherent Verdi V10 + Mira 900F femtosecond laser system, BS – beam splitter, M – mirrors, D-line – dispersive delay line (conventional prism compressor consisting of a SF11 prism pair with a reverse mirror), TD – temporal delay, fiber – Newport F-SPF PP@820 nm, SFG – BBO crystal for SFG, OSA – optical spectrum analyzer.

The technique of SFG-spectral compression, as compared to XFROG, is more efficient, providing sharper spectral signal in a wider spectral (and temporal) range. The temporal delay between the SFG-interacting pulses in the range of ± 16 ps results in a ± 20 nm wavelength shift for the 22 times SFG-spectrally compressed signal (down to 0.12 nm at 400 nm central wavelength), corresponding to the chirp measurement of similariton in the span range of 160 nm (75 THz) at 800 nm central wavelength. This 3D pattern completely

characterizes the generated broadband similariton. Its projections represent the temporal and spectral profiles of the intensity $I(t)$ and $I(\lambda)$, and the curve $\lambda(t)$ connected with the chirp $\omega(t) = \dot{\phi}_f(t)$, as well as with the derivative of spectral phase $\dot{\phi}_f(\omega)$, according to the spectrotemporal similarity of broadband similariton described by Eqs. (2') and (4). In general, through the Fourier transformation of complex temporal amplitude, given by the measured temporal pulse and chirp, the spectral complex amplitude and afterwards the spectral phase could be retrieved. For our case of the broadband similariton, the Eq. (2') permits to have the spectral phase information by a simple scaling $\omega = Ct$, and we have $\dot{\phi}_f(\omega) \approx -\dot{\phi}_f(t) / C$ for the derivative of spectral phase.

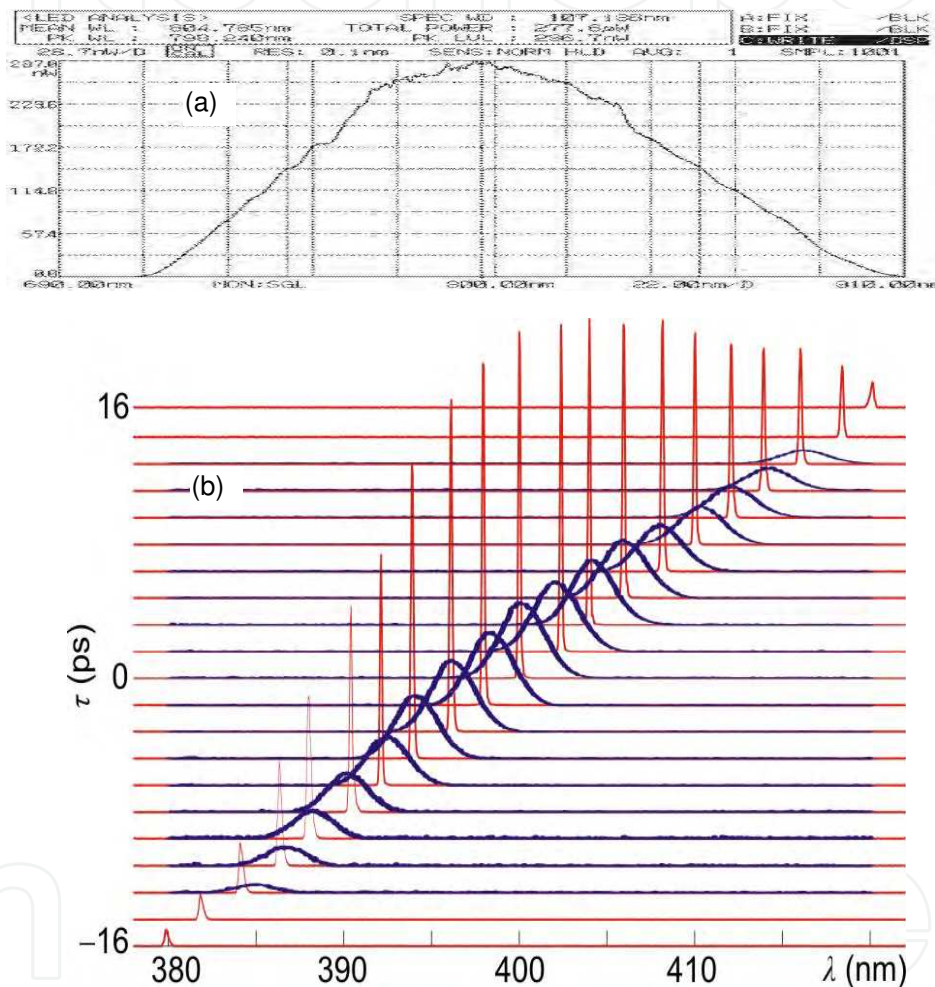


Fig. 9. (a) Measured spectrum of broadband similariton, and (b) 3D frequency tuning patterns with spectral compression (sharp peaks) and without it (thick lines) for the chirp measurement: the 40 nm (75 THz) frequency tuning at 400 nm is adequate to the 160 nm spectral range of similariton at 800 nm for the 32 ps range of temporal delay between SFG-interacting pulses.

Fig. 10 shows the $\dot{\phi}_f(\omega)$ curve obtained this way. It is described by the polynomial $\dot{\phi}_f(\omega) = -15.06 \times 10^3 \text{ fs}^3 \times \omega^2 - 81.13 \times 10^3 \text{ fs}^2 \times \omega$. The quadratic component of $\dot{\phi}_f(\omega)$ is shown separately (inset). The circles in Fig. 10 are the measured experimental points; the dashed and solid curves are for the linear and parabolic fits, respectively.

Concluding, we generated nonlinear-dispersive similariton of 50 THz bandwidth, and carried out its complete characterization through the chirp measurement, using the technique of frequency tuning in the SFG-spectral compression. Our studies state that only fiber dispersion determines the phase (chirp) of broadband nonlinear-dispersive similariton. The fiber TOD results in the same additional phase for broadband nonlinear-dispersive similariton and spectron. The $\sim 1\%$ accuracy of the linear fit for the chirp of the 50-THz bandwidth similariton gives the range of applications for aberration-free similariton-based spectrotemporal imaging [22] and spectral interferometry [45-47]. The described approach to the generation and characterization of broadband similariton can be helpful also for its applications in pulse compression [40,41] and CARS microscopy [51]. For these applications, the low value of TOD can impact significantly and it should be considered more carefully.

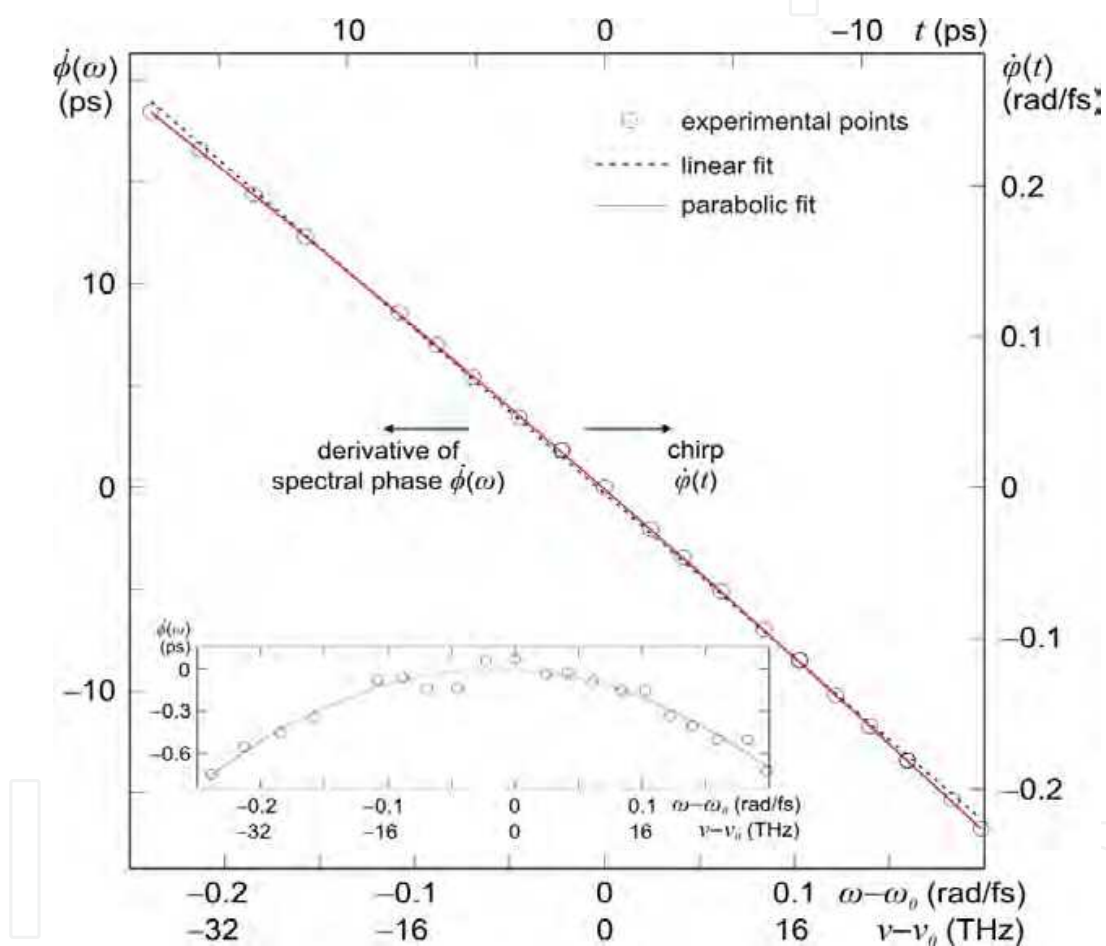


Fig. 10. Broadband similariton's chirp $\dot{\phi}_f(t)$ and derivative of spectral phase $\dot{\phi}_f(\omega)$ with its quadratic component, separately (inset). The $\sim 1\%$ difference from the linear fit in the range of ~ 50 THz gives the range of applications for the similariton-based methods of signal characterization (Section 4).

4. Similariton based self-referencing spectral interferometry for femtosecond pulse characterization

Our studies on broadband similariton serve as a basis for development of a novel method of similariton-based of SI for the femtosecond pulse complete characterization. Below we

present its demonstration in comparison with the method of pulse spectrotemporal imaging in the similariton-induced temporal lens. Application of similariton to the reference-based methods upgrades them up to the self-referencing ones, substantially improving their performance due to the enlarged application range along with the simplicity of the principle and configuration.

Our experimental study of nonlinear-dispersive similariton, described in sec. 2.2, as a remarkable example for the demonstration-application of SI-approach, clearly shows that the classic SI provides accurate measurement with a rather simple setup, but its application range is restricted by the bandwidth of the reference. As mentioned above, the SI characterization of a signal that has undergone a nonlinear interaction with medium requires a special broadband reference to fully cover the broadened signal spectrum. To avoid this restriction, the self-referencing methods of spectral shearing interferometry, such as SPIDER [3] and SPIRIT [4], are developed. This improvement promotes the SI to the class of the most popular and commercialized methods of accurate measurements on the femtosecond time scale, making it compatible with the FROG [1] and MIIPS [6] techniques, at the expense of a more complicated optical arrangement. Our proposed method of similariton-based SI, along with its self-referencing performance, keeps the simplicity of the principle and configuration of the classic SI.

Describing the principle of *similariton-based SI*, for its implementation the setup of Fig. 8 is used, removing the nonlinear BBO crystal and D-line. Splitting the signal beam, its part is injected into a fiber to generate the nonlinear-dispersive similariton-reference, with the complex spectral amplitude $\tilde{A}(f, \omega) = |\tilde{A}(f, \omega)| \exp[i\phi(f, \omega)]$. The residual part of the signal of a complex spectral amplitude $\tilde{A}(0, \omega) = |\tilde{A}(0, \omega)| \exp[i\phi(0, \omega)]$, is coupled with the similariton in a spectrometer with an appropriate time delay. The spectral fringe pattern $S_{SI}(\omega) = 2|\tilde{A}(0, \omega)| |\tilde{A}(f, \omega)| \cos[\phi(0, \omega) - \phi(f, \omega)]$, on the background of the signal and similariton spectra, completely covers the signal spectrum $S(0, \omega) = |\tilde{A}(0, \omega)|^2$, and the whole phase information becomes available, for any signal. The known spectral phase of the similariton-reference allows to retrieve the signal spectral phase $\phi(0, \omega)$, and by measuring also the signal spectrum, to reconstruct the complex temporal amplitude $A(0, t)$ of the signal through Fourier transformation. Thus, the method of similariton-based SI joins the advantages of both the classic SI [2] and spectral shearing interferometry [3-5], combining the simplicity of the principle and configuration with the self-referencing performance. Examining the similariton-based SI, we compare its measurements with the ones carried out by a prototype of the femtosecond oscilloscope (FO) based on the pulse spectrotemporal imaging in the similariton-induced temporal lens in the SFG process. Our comparative study, involving also theoretical and autocorrelation check, along with the demonstration and study of the similariton-based SI, serves also for the inspection of the prototype of similariton-based FO, the measurements of which previously were compared with the autocorrelation only [22].

The method of SFG-*spectrotemporal imaging* for direct femtosecond scale measurements is based on the conversion of temporal information to the spectral domain in a similariton-induced parabolic temporal lens [22,46,47]. The setup of the similariton-based SI is modified to FO by replacing the temporal delay (TD) with a dispersive delay line (D-line) and placing

a nonlinear crystal for SFG at the system output (returning to the initial configuration of Fig. 8). In the spectral domain, the dispersive delay works as a parabolic phase modulator, and the signal $\tilde{A}(0, \omega)$ passed through is described as $\tilde{A}(d, \omega) = \tilde{A}(0, \omega) \exp(i\ddot{\phi}_d \omega^2 / 2)$, with the given coefficient $\ddot{\phi}_d \approx -C_d^{-1}$. In the fiber arm, we have a nonlinear-dispersive similariton with the known parameters as in the case of similariton-based SI. In both arms of the setup, we have practically linearly chirped pulses, and the temporal and spectral complex amplitudes repeat each other in the temporal Fraunhofer zone, i.e. spectron pulses are formed [47]: $A(d, t) \propto \tilde{A}(d, \omega)$, and $A(f, t) \propto \tilde{A}(f, \omega)$ with $\omega = C_{d,f} t$. Under the conditions of the opposite and same value chirps $C_f = -C_d \equiv C$, and constant similariton spectrum throughout the signal spectrum, the output temporal SFG-signal repeats the input spectral amplitude: $A_{SFG}(t) \propto A(d, t) \times A(f, t) \propto \tilde{A}(0, \omega)$. Accordingly, the output spectral and input temporal amplitudes repeat each other $\tilde{A}_{SFG}(\omega) \propto A(0, t)$, and the output SFG-spectrum displays directly the input temporal pulse: $S_{SFG}(\omega) = |\tilde{A}_{SFG}(\omega)|^2 \propto |A(0, t)|^2 = I(0, t)$, with the scale $\omega = Ct$. The resolution of such a similariton-based FO is given by the transfer function of the similariton's spectrum [22,47], and FO with a similariton-reference of the bandwidth of a few tens of nanometers provides the direct measurement of temporal pulse in a spectrometer, exceeding the resolution of the achievement of silicon-chip-based ultrafast optical oscilloscope [21] by an order of magnitude.

In the *experiment*, different amplitude- and phase-modulated pulses at the setup input are shaped and the signal radiation is split by a beam-splitter (80% + 20%). The low-power part is directed to the TD or D-line (SF 11 prism pair with the reverse mirror) for similariton-based SI and spectrotemporal imaging, respectively. In the second path, the high-power pulse (with average power of up to 500 mW) is injected into a standard single-mode fiber (1.65 m Newport F-SPF PP@820 nm) by a microscope objective (10×) to generate broadband nonlinear-dispersive similaritons. For the SI-measurements, these two pulses are coupled directly into the OSA and the SI fringe pattern and signal spectrum are registered. To retrieve the spectral phase, the Fourier-transform algorithm of the fringe-pattern analysis are used [44-47]. For the FO-measurements, a BBO crystal at the input of OSA is placed, and the SFG-spectrotemporal image is registered directly. The similariton-based SI and FO measurements are carried out together with the autocorrelation check by a standard APE PulseCheck autocorrelator.

First, the similariton-based SI for the laser pulses stretched and chirped in SF11 glasses of different thickness is tested, comparing the results with the autocorrelation measurements (Fig. 11). For the dispersion-induced parabolic spectral phases of the stretched pulses, the coefficients of the dispersion-induced parabolic spectral phases [Fig. 11(a)] are the following: $\alpha \equiv \phi''(\omega) = 1.94 \times 10^{-3}$, 4.94×10^{-3} , 6.34×10^{-3} , and 10.78×10^{-3} ps² for the 0, 2, 3, and 5-cm glasses, respectively. The SI-reconstructed pulses, correspondingly, have durations of 108, 197, 252, and 365 fs, in a good accordance with the autocorrelation durations of 156, 298, 369 and 539 fs of the measurements shown in Fig. 11(b).

Afterwards, measurements for multi-peak pulses are carried out together with the autocorrelation check. The SI calibrating measurement of the α coefficient for similariton, using the known laser pulse as a reference, gives the value $\alpha = 2.1 \times 10^4$ fs², in accordance with the

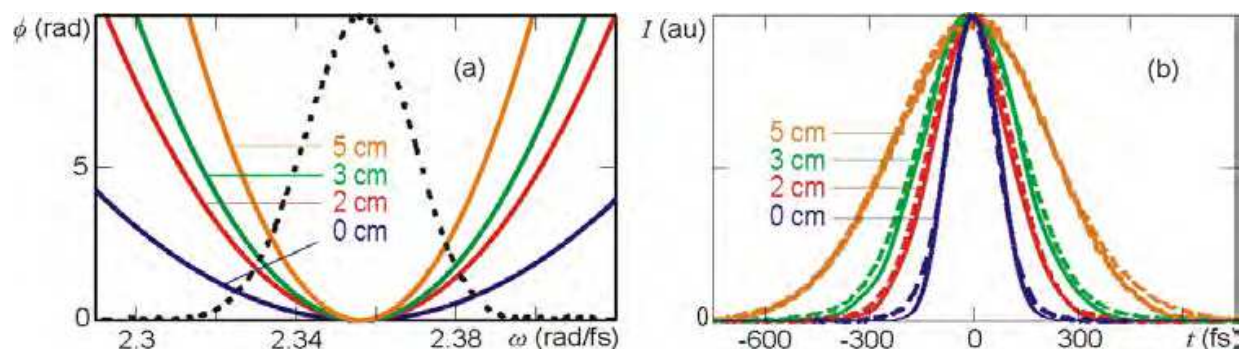


Fig. 11. Similariton-based SI for pulses dispersively stretched and chirped in SF11 glasses of different thickness: (a) retrieved spectral phases with the measured spectrum (dotted line), and (b) autocorrelation functions of SI-reconstructed temporal pulses (solid) in comparison with autocorrelation traces measured (dashed).

expression $\alpha = \beta_2 f$ with the values $f = 49$ cm and $\beta_2 = 40$ fs²/mm ($D_\lambda = -103$ ps/nm/km at the wavelength 850 nm, according to the data provided by the fiber manufacturer). Then different multi-peak signal pulses are shaped inserting thin glass plates in parts of the beam. The beam parts passed through the plates obtain time delay with respect to the free-propagated part. The movement of the plates along the vertical axis adjusts the power proportion among the peaks. The thicknesses of the plates give the time delay between the peaks; e.g. a 0.12 mm thick glass plate gives a 200 fs delay, if assuming the refractive index of the plate equal to 1.5. Using double- and triple- peak signal pulses, we carry out SI-measurements and compare the results with measured autocorrelation tracks.

The application range and limitations of similariton-based SI are conditioned by the parameters of input radiation and fiber, which are necessary to generate the similariton-reference with parabolic phase. Fig. 12 and 13 illustrate the experiment for the typical regime preceding the similariton shaping: results for double- and triple-peak signal pulses are shown. As Fig. 12 illustrates, having the spectrum (b, black) and SI-retrieved spectral phase (b, blue solid line) of pulse, its temporal profile (c, blue solid line) is reconstructed through Fourier transformation. To check the precision of our measurements through similariton-based SI, we calculate the autocorrelation of reconstructed pulse (d, blue solid line) and compare it with the intensity autocorrelation measured at the input of the system (d, black). The spectral shape of nonlinear-dispersive similariton (a) ensures the fulfillment of necessary conditions for the parabolicity of the spectral phase of similariton (according to [23]). The structure of the similariton spectrum (a), strange at first glance, is typical for short lengths of nonlinear-dispersive interaction, and is observed also for parabolic similaritons generated in fiber amplifiers [52]. The blue solid and red dashed curves in Fig. 12 correspond to the pulse reconstruction with the spectral phase coefficients $\alpha = 2.1 \times 10^4$ fs² and $\alpha = 1.995 \times 10^4$ fs² (5% difference), respectively. Fig. 13 shows the analogue procedures for a pulse with more complex sub-structure.

Finally, we compare the measurements of the similariton-based SI and FO, together with a theoretical check. The double-peak signal pulses are shaped with the spectral domain amplitude- and phase-modulation given by the peaks' temporal distance T and their proportion μ . The temporal amplitude $A(t) = A_0(t) + \mu A_0(t + T)$ corresponds to the complex

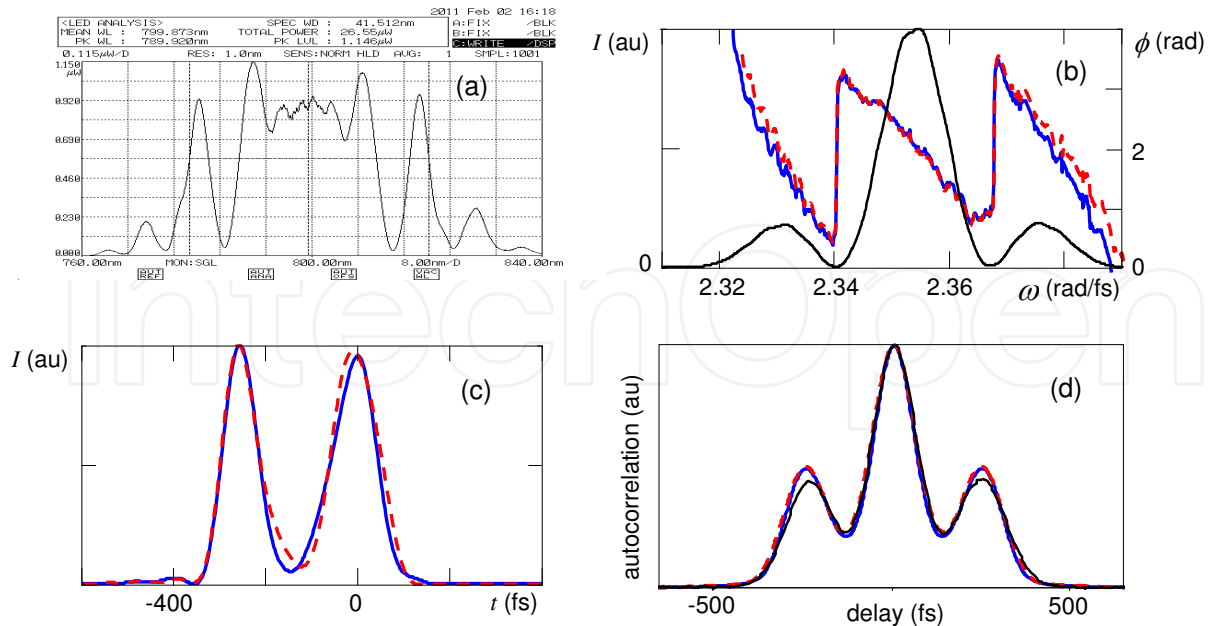


Fig. 12. Reconstruction of double-peak pulse (shaped by means of a 130- μm thick glass) through similariton-based SI in comparison with autocorrelation measurement: (a) spectrum of nonlinear-dispersive similariton; (b) retrieved spectral phase and measured spectrum; (c) reconstructed pulse temporal profile; and (d) autocorrelation tracks. Blue solid and red dashed curves are for $\alpha = 2.1 \times 10^4 \text{ fs}^2$ and $\alpha = 1.995 \times 10^4 \text{ fs}^2$ (5% difference), respectively, and the black one in (d) is the measured autocorrelation track.

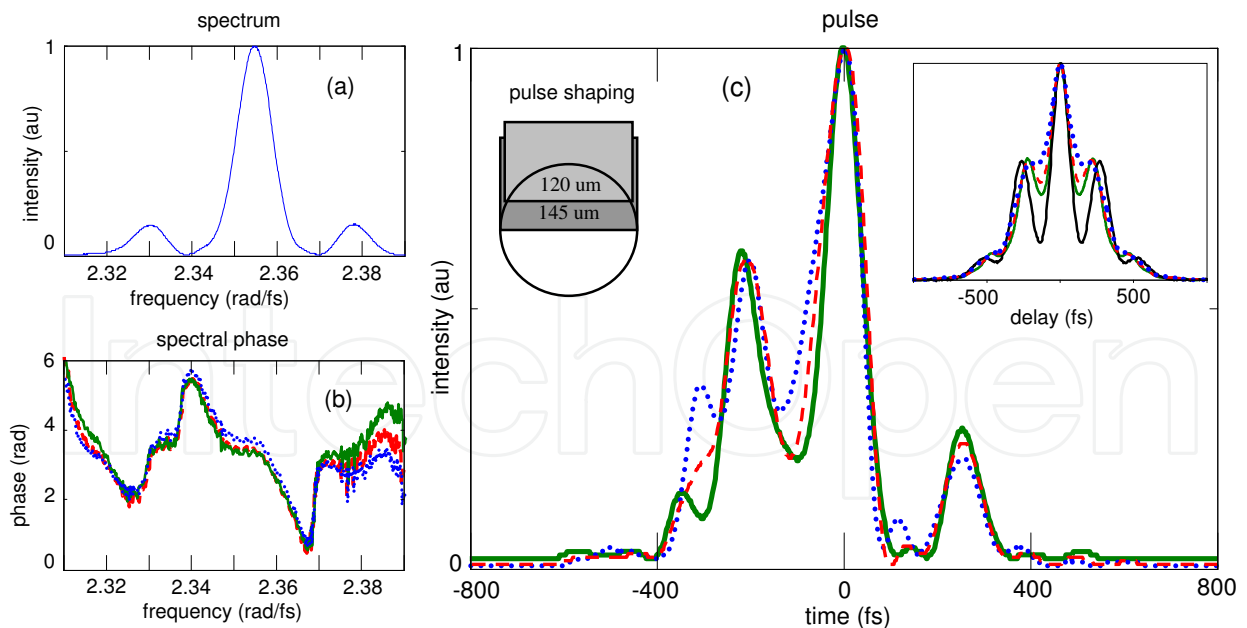


Fig. 13. Reconstruction of three-peak pulse (shaped by means of 145 and 120- μm thick glasses) through similariton-based SI in comparison with autocorrelation: (a) measured spectrum; (b) retrieved spectral phases; (c) reconstructed pulse temporal profiles and autocorrelation tracks (inset). Blue dotted, red dashed and green solid curves are for $\alpha = 2.1 \times 10^4 \text{ fs}^2$, $1.995 \times 10^4 \text{ fs}^2$, and $1.89 \times 10^4 \text{ fs}^2$, respectively, and the black one of the inset is the measured autocorrelation.

spectral amplitude $\tilde{A}(\omega) = \tilde{A}_0(\omega)\rho(\omega)\exp[i\phi(\omega)]$, with the $\rho(\omega) = \sqrt{1 + \mu^2 + 2\mu\cos(\omega T)}$ amplitude- and $\phi(\omega) = \arctan[(\sin \omega T) / (\mu^{-1} + \cos \omega T)]$ phase-modulation. To shape such double-peak pulses, the laser beam is expanded and a thin glass plate in its part is placed, as described above. The thickness of the plate gives the time delay between the peaks; e.g. a 0.12 mm thick glass plate gives a 200 fs delay, according to autocorrelation check. The similariton-based SI and FO are comparatively experimented using the double-peak signal pulse: the SI-reconstructed pulses are compared with spectrotemporal images of the signal.

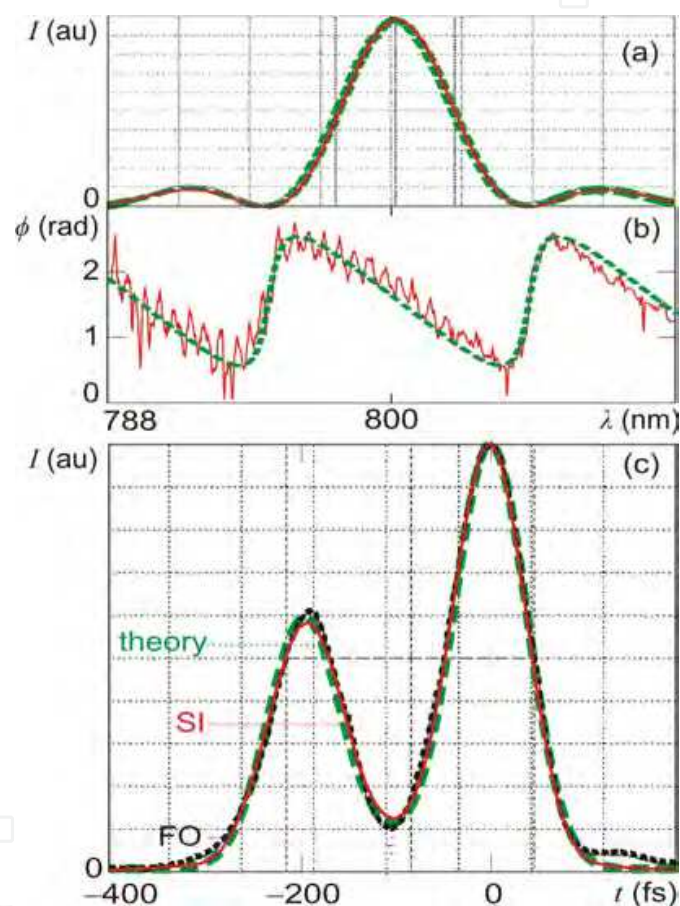


Fig. 14. Comparison of similariton-based SI and FO for a double-peak signal pulse: (a) measured spectrum, (b) retrieved spectral phase, and (c) pulse. Dashed, solid and dotted curves are for the theory, similariton-based SI and FO, respectively.

Fig. 14 illustrates this experiment by the results for a double-peak signal pulse: the quantitative accordance of the measured spectrum (a) and retrieved spectral phase (b) with the theoretical curves (dashed) leads to an accurate pulse reconstruction through similariton-based SI (c, solid). An accurate spectrotemporal imaging (c, dotted) is ensured by the similariton of the bandwidths of ≥ 40 nm. The differences between these independent SI- and FO-measurements and theoretical curve are hardly seen, evidencing both the accuracy of the mentioned measurements and the potential of similariton-based methods.

Obviously, the demonstrated methods of femtosecond signal characterization can be implemented also by the use of “standard” parabolic similaritons generated in active or dispersion decreasing fibers. In a recent progress in the generation of parabolic broadband similaritons, bandwidths of up to 11 THz (40 nm at 1050 nm central wavelength) are achieved [52]. However, the use of the nonlinear-dispersive similariton generated in a piece of standard passive fiber currently is more beneficial, providing larger bandwidths and thus larger application ranges with technically simpler experimental arrangement.

Thus, the methods of similariton-based SI and spectrotemporal imaging are experimentally demonstrated as two applications of similariton. The reference-based methods become self-referencing by the use of similariton. The described comparative study, involving also theoretical check and autocorrelation measurements, ensures the quantitative accordance and high precision of both the similariton-referencing methods. While the method of similariton-based spectrotemporal imaging has the advantage of direct pulse measurement, and thus leads to the development of a femtosecond optical oscilloscope, it does not give phase information. The method of similariton-based SI provides the complete (amplitude and phase) characterization of femtosecond signal. The method of similariton-based SI provides the complete (amplitude and phase) characterization of femtosecond signal.

5. Conclusion

Our spectral interferometric studies demonstrate the spectronic nature and distinctive properties of nonlinear-dispersive similariton, of up to 5-THz bandwidth, generated in a passive fiber. The key property of nonlinear-dispersive similariton of having a parabolic phase (linear chirp), given by the fiber dispersion only, leads to its spectrotemporal similarity and thus to its self-spectrotemporal imaging, with the accuracy given by spectral broadening and pulse stretching together.

Generating similaritons of 50-THz bandwidth, we carry out their complete characterization through the chirp measurement, using the technique of frequency tuning in the process of spectral compression by sum-frequency generation. The studies permit to generalize the description of nonlinear-dispersive similaritons, verifying that only fiber dispersion determines the phase (chirp) of such broadband similaritons. The third order dispersion of fiber results in the same additional phase for broadband nonlinear-dispersive similariton and spectron. The ~1% accuracy of the linear fit for the chirp of the 50-THz bandwidth similariton gives the range of applications for aberration-free similariton-based spectrotemporal imaging and spectral interferometry. The described approach to the generation and characterization of broadband similariton can be helpful also for its applications in pulse compression and CARS microscopy.

We develop and implement a similariton based self-referencing method of spectral interferometry for the complete characterization of femtosecond signal. The method is based on the similariton generation from the part of signal and its use as a reference for the interference with the signal in the spectrometer. Therefore, the method of similariton-based spectral interferometry combines the advantage of the simple principle and configuration with the self-referencing performance. We experiment the similariton-based method of spectral interferometry in comparison with the measurements carried out with the prototype of femtosecond oscilloscope based on the spectrotemporal imaging in a

similariton-induced temporal lens. Our comparative study, carried out together with theoretical check and autocorrelation measurements, evidences the quantitative accordance and high precision of both the similariton-referencing methods of spectral interferometry and spectrotemporal imaging for accurate femtosecond-scale temporal measurements. The similariton-based spectrotemporal imaging has the advantage of direct pulse measurement leading to the development of a femtosecond optical oscilloscope, but it does not give the phase information without additional interferometric measurement. The novel method of similariton-based spectral interferometry, with a rather simple setup and self-referencing performance, provides the complete (amplitude and phase), high-resolution characterization of femtosecond signal.

6. Acknowledgments

The work was carried out within the framework of the 978027 project of Science for Peace Programme of North Atlantic Treaty Organization, collaborative programme project IE007 of Centre National de la Recherche Scientifique (CNRS), France – State Committee of Science (SCS), Armenia, and ANSEF grant # PS-opt-2903. A. Zeytunyan also acknowledges SCS, National Foundation of Science and Advanced Technology (NFSAT), and Civilian Research and Development Foundation (CDRF) for financial support in the framework of the Early Career Support Program (grant numbers A-16 and ECSP-09-50).

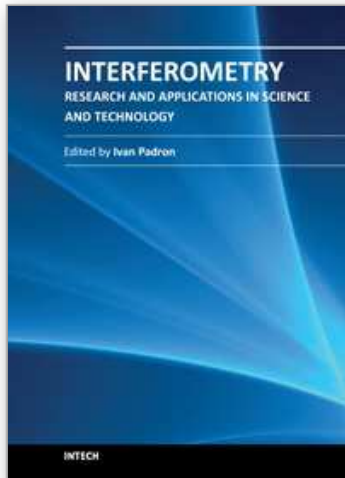
7. References

- [1] D.J.Kane, R.Trebino “Single-shot measurement of the intensity and phase of an arbitrary ultrashort pulse by using frequency-resolved optical gating” *Opt.Lett.*18, 823–825 (1993).
S. Akturk, M. Kimmel, P. O’Shea, R. Trebino “Measuring spatial chirp in ultrashort pulses using singleshot frequency-resolved optical gating” *Opt. Express* 11, 68–78 (2003).
- [2] J. Piasecki, B. Colombeau, M. Vampouille, C. Froehly, J.A. Arnaud, “Nouvelle méthode de mesure de la réponse impulsionnelle des fibres optiques,” *Appl. Opt.* 19, 3749 (1980).
F. Reynaud, F. Salin, and A. Barthélémy, “Measurement of phase shifts introduced by nonlinear optical phenomena on subpicosecond pulses,” *Opt. Lett.* 14, 275–277 (1989).
- [3] C. Iaconis and I. A. Walmsley, “Spectral phase interferometry for direct electric-field reconstruction of ultrashort optical pulses,” *Opt. Lett.* 23, 792–794 (1998).
- [4] V.Messenger, F.Louradour, C.Froehly, A.Barthélémy “Coherent measurement of short laser pulses based on spectral interferometry resolved in time” *Opt.Lett.*28, 743–745 (2003).
M. Lelek, F. Louradour, A. Barthélémy, C. Froehly, T. Mansourian, L. Mouradian, J.-P. Chambaret, G. Chériaux, B. Mercier, “Two-dimensional spectral shearing interferometry resolved in time for ultrashort optical pulse characterization,” *J. Opt. Soc. Am. B* 25, A17–A24 (2008).

- [5] P.Kockaert, M.Haelterman, Ph.Emplit, C.Froehly, "Complete characterization of (ultra)-short optical pulses using fast linear detectors," *IEEE J. Sel.Top.Quantum Electron.* 10, 206–212 (2004).
- [6] V.V. Lozovoy, I. Pastirk, M. Dantus, "Multiphoton intrapulse interference. IV. Ultrashort laser pulse spectral phase characterization and compensation," *Opt. Lett.* 29, 775 (2004).
- B.Xu, J.M.Gunn, M.Dela Cruz, V.V.Loizovoy, M.Dantus "Quantitative investigation of the multiphoton intrapulse interference phase scan method for simultaneous phase measurement and compensation of femtosecond laser pulses" *J.Opt.Soc.Am. B* 23, 750–759 (2004).
- [7] M. C. Nuss, M. Li, T. H. Chiu, A. M. Weiner, A. Partovi, "Time-to-space mapping of femtosecond pulses," *Opt. Lett.* 19, 664–666 (1994).
- [8] P.C.Sun, Y.T.Mazurenko, Y.Fainman, "Femtosecond pulse imaging: ultrafast optical oscilloscope," *J. Opt. Soc. Am. A* 14, 1159–1170 (1997).
- [9] C.V.Bennett, B.H.Kolner, "Upconversion time microscope demonstrating 103_ magnification of femtosecond waveforms," *Opt. Lett.* 24, 783–785 (1999).
- [10] M.Vampouille, A.Barthélémy, B.Colombeau, C.Froehly "Observation et applications des modulations de fréquence dans les fibres unimodales" *J. Opt. (Paris)* 15, 385–390 (1984).
- [11] M. Vampouille, J. Marty, C. Froehly, "Optical frequency intermodulation between two picosecond laser pulses," *IEEE J. Quantum Electron.* 22, 192–194 (1986).
- [12] M. T. Kauffman, W. C. Banyai, A. A. Godil, D. M. Bloom, "Time-to-frequency converter for measuring picosecond optical pulses," *Appl. Phys. Lett.* 64, 270–272 (1994).
- [13] J. Azana, N. K. Berger, B. Levit, B. Fischer, "Time-tofrequency conversion of optical waveforms using a single time lens system," *Phys. Scr. T118*, 115–117 (2005); *IEEE Photon. Technol. Lett.* 16, 882–884 (2004); *Opt. Commun.* 217, 205–209 (2003).
- [14] E.Arons, E.N.Leith, A.Tien, R.Wagner, "Highresolution optical chirped pulse gating," *Appl. Opt.* 36, 2603–2608 (1997).
- [15] L.Kh.Mouradian, F.Louradour, V.Message, A.Barthélémy, C.Froehly "Spectro-temporal imaging of femtosecond events" *IEEE J. Quantum Electron.* 36, 795–801 (2000).
- [16] L.Kh.Mouradian, A.V.Zohrabian, C.Froehly, F.Louradour, A.Barthélémy "Spectral imaging of pulses temporal profile," in *Conference on Lasers and Electro-Optics (CLEO / Europe)*, OSA Tech. Digest Series, paper CMA5 (1998).
- [17] L.Kh.Mouradian, F.Louradour, C.Froehly, A.Barthélémy "Self- and cross-phase modulation of chirped pulses: spectral imaging of femtosecond pulses" in *Nonlinear Guided Waves and Their Applications*, OSA Tech. Digest Series, v.5, paper NFC4 (1998).
- [18] L.Kh.Mouradian, A.V.Zohrabyan, V.J.Ninoyan, A.A.Kutuzian, C.Froehly, F.Louradour, A.Barthélémy, "Characterization of optical signals in fiber-optic Fourier converter," *Proc. SPIE* 3418, 78–85 (1998).
- [19] A.V.Zohrabyan, A.A.Kutuzian, V.Zh.Ninoyan, L.Kh.Mouradian "Spectral compression of picosecond pulses by means of cross phase modulation" *AIP Conf. Proc.* 406, 395–401 (1997).

- [20] N. L. Markaryan L. Kh. Muradyan, "Determination of the temporal profiles of ultrashort pulses by a fibre-optic compression technique," *Quantum Electron.* 25, 668–670 (1995).
- [21] M.A.Foster, R.Salem, D.F.Geraghty, A.C.Turner-Foster, M.Lipson, A.L.Gaeta, "Silicon-chip based ultrafast optical oscilloscope," *Nature* 456, 81–84 (2008).
- [22] T. Mansuryan, A. Zeytunyan, M. Kalashyan, G. Yesayan, L. Mouradian, F. Louradour, A.Barthélémy, "Parabolic temporal lensing and spectrotemporal imaging: a femtosecond optical oscilloscope," *J. Opt. Soc. Am. B* 25, A101–A110 (2008).
- [23] A.Zeytunyan,G.Yesayan,L.Mouradian, P.Kockaert,P.Emplit, F.Louradour, A.Barthélémy "Nonlinear-dispersive similariton of passive fiber," *J. Europ. Opt. Soc. Rap. Public.* 4, 09009 (2009).
- [24] M.A.Kalashyan, K.A.Palandzhyan, G.L.Esayan, L.Kh.Muradyan "Generation of transform-limited rectangular pulses in a spectral compressor" *Quantum Electron.* 40 (10), 868–872. 2010,
- [25] M.A.Kalashyan, K.H.Palanjyan, T.J.Khachikyan, T.G.Mansuryan, G.L.Yesayan, L.Kh.Mouradian "Prism -Lens Dispersive Delay Line" *Tech.Phys.Lett.* 35 (3), 211–214 (2009).
- [26] J.M.Dudley, C.Finot, D.J.Richardson, G. Millot, "Self-similarity and scaling phenomena in nonlinear ultrafast optics," *Nature Physics* 3, 597–603 (2007).
- [27] C.Finot, J.M.Dudley, B.Kibler, D.J.Richardson, G.Millot, "Optical parabolic pulse generation and applications," *IEEE J. Quantum Electron.* 45, 1482–1489 (2009).
- [28] D.Anderson, M.Desaix, M.Karlson, M.Lisak, M.L.Quiroga-Teixeiro, "Wave-breaking-free pulses in nonlinear optical fibers," *J. Opt. Soc. Am. B* 10, 1185–1190 (1993).
- [29] M.E. Fermann, V.I. Kruglov, B.C. Thomsen, J.M. Dudley, J.D. Harvey, "Self-similar propagation and amplification of parabolic pulses in optical fibers," *Phys. Rev. Lett.* 84, 6010–6013 (2000).
- [30] V.I. Kruglov, A.C. Peacock, J.M. Dudley, J.D. Harvey, "Self-similar propagation of high-power parabolic pulses in optical fiber amplifiers," *Opt. Lett.* 25, 1753–1755 (2000).
- [31] V.I.Kruglov, A.C.Peacock, J.D.Harvey, J.M.Dudley "Self-similar propagation of parabolic pulses in normal-dispersion fiber amplifiers," *J. Opt. Soc. Am. B* 19, 461–469 (2002).
- [32] C. Finot, G. Millot, C. Billet, J.M. Dudley, "Experimental generation of parabolic pulses via Raman amplification in optical fiber," *Opt. Express* 11, 1547–1552 (2003).
- [33] F.Ö. Ilday, J.R. Buckley, W.G. Clark, F.W. Wise, "Self-similar evolution of parabolic pulses in a laser," *Phys. Rev. Lett.* 92, 213902 (2004).
- [34] T. Hirooka, M. Nakazawa, "Parabolic pulse generation by use of a dispersion-decreasing fiber with normal group-velocity dispersion," *Opt. Lett.* 29, 498–500 (2004).
- [35] C. Finot, B. Barviau, G. Millot, A. Guryanov, A. Sysoliatin, S. Wabnitz, "Parabolic pulse generation with active or passive dispersion decreasing optical fibers," *Opt. Express* 15, 15824–15835 (2007).
- [36] A.S.Zeytunyan, K.A.Palandjyan, G.L.Yesayan, L.Kh.Mouradian, "Nonlinear dispersive similariton: spectral interferometric study" *Quantum Electron.* 40, 327–328 (2010).

- [37] A.S.Zeytunyan, K.A.Palanjyan, G.L.Yesayan, L.Kh.Mouradian, "Spectral-interferometric study of nonlinear-spectronic similariton:" J. Contemp. Phys. 45, 64–69 (2010).
- [38] C.Finot, B.Kibler, L.Provost, S.Wabnitz, "Beneficial impact of wave-breaking for coherent continuum formation in normally dispersive nonlinear fibers," J. Opt. Soc. Am. B 25, 1938–1948 (2008).
- [39] A.S.Zeytunyan, H.R.Madatyan, G.L.Yesayan, L.Kh.Mouradian "Diagnostics of femto-second laser pulses based on generation of nonlinear-dispersive similariton" J. Contemp. Phys. 45, 169–171 (2010).
- [40] V.I. Kruglov, D. Méchin, J.D. Harvey, "High compression of similariton pulses under the influence of higher-order effects," J. Opt. Soc. Am. B 24, 833–838 (2007).
- [41] K.Palanjyan, A.Muradyan, A.Zeytunyan, G.Yesayan, L.Mouradian, "Pulse compression down to 17 femtoseconds by generating broadband similariton," Proc. SPIE 7998, 79980N (2010).
- [42] C. Finot, G. Millot "Synthesis of optical pulses by use of similaritons" Opt. Express 12, 5104–5109 (2004).
- [43] A.Zeytunyan, G.Yesayan, L.Mouradian, F.Louradour, A.Barthélémy, "Applications of similariton in ultrafast optics: spectral interferometry and spectrotemporal imaging," in *Frontiers in Optics*, OSA Tech. Digest, paper FWI5 (2009).
- [44] A.Zeytunyan, A. Muradyan, G. Yesayan, L. Mouradian, "Broadband similariton" Laser Physics 20, 1729–1732 (2010).
- [45] A.Zeytunyan, A.Muradyan, G.Yesayan, L.Mouradian, F.Louradour, A.Barthélémy "Measuring of Broadband Similariton Chirp" Nonlinear Photonics OSA Tech. Digest, paper NME46 (2010).
- [46] A.Zeytunyan, A.Muradyan, G.Yesayan, L.Mouradian, F.Louradour, A.Barthelemy, Similariton for Femtosecond Optics Proc. ECOC 2010 (19-23 Sep. 2010), Torino, Italy, paper Mo.2.E.5 (2010).
- [47] A.Zeytunyan, A.Muradyan, G.Yesayan, L.Mouradian, F.Louradour, A.Barthélémy "Generation of broadband similaritons for complete characterization of femtosecond pulses" Opt. Commun. v. 284, pp. 3742–3747 (2011).
- [48] A.M. Heidt, "Pulse preserving flat-top supercontinuum generation in all-normal dispersion photonic crystal fibers," J. Opt. Soc. Am. B 27, 550–559 (2010).
- [49] D.T. Reid, P. Loza-Alvarez, C.T.A. Brown, T. Beddard, W. Sibbett, "Amplitude and phase measurement of mid-infrared femtosecond pulses by using cross-correlation frequency-resolved optical gating," Opt. Lett. 25, 1478–1480 (2000).
- [50] J. Dudley, X. Gu, L. Xu, M. Kimmel, E. Zeek, P. O'Shea, R. Trebino, S. Coen, R. Windeler, "Cross-correlation frequency resolved optical gating analysis of broadband continuum generation in photonic crystal fiber: simulations and experiments," Opt. Express 10, 1215–1221 (2002).
- [51] A.F. Pegoraro, A. Ridsdale, D.J. Moffatt, Y. Jia, J.P. Pezacki, A. Stolow, "Optimally chirped multimodal CARS microscopy based on a single Ti:sapphire oscillator," Opt. Express 17, 2984–2996 (2009).
- [52] W.H. Renninger, A. Chong, F.W. Wise, "Self-similar pulse evolution in an all-normal-dispersion laser," Phys. Rev. A 82, 021805(R) (2010).



Interferometry - Research and Applications in Science and Technology

Edited by Dr Ivan Padron

ISBN 978-953-51-0403-2

Hard cover, 462 pages

Publisher InTech

Published online 21, March, 2012

Published in print edition March, 2012

This book provides the most recent studies on interferometry and its applications in science and technology. It is an outline of theoretical and experimental aspects of interferometry and their applications. The book is divided in two sections. The first one is an overview of different interferometry techniques and their general applications, while the second section is devoted to more specific interferometry applications comprising from interferometry for magnetic fusion plasmas to interferometry in wireless networks. The book is an excellent reference of current interferometry applications in science and technology. It offers the opportunity to increase our knowledge about interferometry and encourage researchers in development of new applications.

How to reference

In order to correctly reference this scholarly work, feel free to copy and paste the following:

Levon Mouradian, Aram Zeytunyan and Garegin Yesayan (2012). Similariton-Based Spectral Interferometry for Signal Analysis on Femtosecond Time Scale, Interferometry - Research and Applications in Science and Technology, Dr Ivan Padron (Ed.), ISBN: 978-953-51-0403-2, InTech, Available from: <http://www.intechopen.com/books/interferometry-research-and-applications-in-science-and-technology/similariton-based-spectral-interferometry-for-signal-analysis-on-femtosecond-time-scale>

INTECH
open science | open minds

InTech Europe

University Campus STeP Ri
Slavka Krautzeka 83/A
51000 Rijeka, Croatia
Phone: +385 (51) 770 447
Fax: +385 (51) 686 166
www.intechopen.com

InTech China

Unit 405, Office Block, Hotel Equatorial Shanghai
No.65, Yan An Road (West), Shanghai, 200040, China
中国上海市延安西路65号上海国际贵都大饭店办公楼405单元
Phone: +86-21-62489820
Fax: +86-21-62489821

© 2012 The Author(s). Licensee IntechOpen. This is an open access article distributed under the terms of the [Creative Commons Attribution 3.0 License](#), which permits unrestricted use, distribution, and reproduction in any medium, provided the original work is properly cited.

IntechOpen

IntechOpen